Materials Science and Engineering A 539 (2012) 38–41

Contents lists available at SciVerse ScienceDirect

Materials Science and Engineering A

journal homepage: www.elsevier.com/locate/msea

The effects of alloying elements on generalized stacking fault energies, strength and ductility of γ'-Ni_3Al

Xiao-Xiang Yu [a,b], Chong-Yu Wang [b,c,*]

[a] Department of Material Science and Engineering, Tsinghua University, Beijing 100084, China
[b] Department of Physics, Tsinghua University, Beijing 100084, China
[c] The International Centre for Materials Physics, Chinese Academy of Sciences, Shenyang 110016, China

ARTICLE INFO

Article history:
Received 17 September 2011
Accepted 19 December 2011
Available online 18 January 2012

Keywords:
Ni-based superalloys
First-principles
Strengthening
Alloying elements

ABSTRACT

Using first-principles calculations, we study the effects of the alloying elements Re, Ta, W, Ru and Ti on the generalized stacking fault energies, strength and ductility of γ'-Ni_3Al. The element Re effectively increases three kinds of generalized stacking fault energies on the (1 1 1) plane inducing more strength and less ductility of Ni_3Al than the other elements. Quantificational analyses of bonding strength between alloying elements and their neighbor atoms reveal the electronic mechanism underlying these effects.

1. Introduction

Nickel-based single-crystal superalloys are widely used structural materials in turbine engines due to their superior high-temperature mechanical properties [1]. The main structure of these alloys is the precipitation of the ordered γ'-Ni_3Al phase with $L1_2$ structure, which is coherently embedded in a solid solution matrix of the γ-Ni phase. γ'-Ni_3Al, with its anomalous temperature dependence of the yield stress, is largely responsible for the strength of superalloys and their resistance to deformation at high temperatures [2,3]. Therefore, a study of the mechanical behaviors of γ'-Ni_3Al should partially reflect the global properties of Ni-based superalloys.

The configuration and movement of dislocations play a key role in understanding plastic deformation and mechanical properties of crystalline solids. One example is the existence of glissile and sessile configurations of the $\langle\bar{1}\,0\,1\rangle\{1\,1\,1\}$ dislocation in Ni_3Al leading to the anomalous yield behavior [4–6]. One perfect $\langle\bar{1}\,0\,1\rangle\{1\,1\,1\}$ dislocation in Ni_3Al will dissociate into two partial $a/2\langle\bar{1}\,0\,1\rangle\{1\,1\,1\}$ dislocations containing an anti-phase boundary(APB) fault, as Fig. 1 shows. The $a/2\langle\bar{1}\,0\,1\rangle\{1\,1\,1\}$ dislocation will further dissociate into two $a/6\langle\bar{1}\,\bar{1}\,2\rangle(1\,1\,1)$ Shockley partial dislocations separated by complex stacking faults (CSF). The $\langle\bar{1}\,0\,1\rangle\{1\,1\,1\}$ dislocation will also dissociate into two $a/3\langle\bar{2}\,1\,1\rangle(1\,1\,1)$ dislocations bounding a superlattice intrinsic stacking fault (SISF).

Fundamentally, the large-scale properties of materials can be traced to the small scale [7,8]. Plastic deformation on the macroscopic scale is influenced by electronic structure (or bonding) on the atomic scale. In the Peierls–Nabarro model, the core structures and properties of dislocations in many materials [9–12] have been investigated by combining density functional theory (DFT) with elasticity theory using the concept of generalized-stacking fault (GSF) energy (or |Ã surface) introduced by Vitek [13,14]. In addition, Rice [15–18] introduced the unstable stacking fault energy, γ_{us}, to evaluate brittle vs. ductile response in fcc and bcc metals in terms of the competition between dislocation nucleation and Griffith cleavage at a crack tip. γ_{us} is the maximum energy encountered on the GSF energy surface during rigid sliding along a slip plane, in the Burgers vector direction. Parameters for the GSF energy surface obtained from DFT calculations can also be used to evaluate twinnabilities in nanocrystalline metals [8,19–21]. Therefore, GSF energies contain many important solid-state parameters, which bridge the gap between electronic structures and dynamics of dislocations.

To acquire extraordinary properties, more than 10 alloying elements are added to nickel-based single-crystal superalloys, including Co, Cr, Ti, Ta, Mo, W, Re and Ru. Experimental results [22–24] have confirmed that the elements Ta and Ti preferentially partition to the γ'-Ni_3Al in superalloys, whereas W distributes averagely between two phases. Besides, although Re and Ru preferentially partition to the γ-Ni, some Re and Ru still enter into the γ'-Ni_3Al. The effects of these elements on the GSF energies of γ'-Ni_3Al are still unclear. The abilities of these elements altering

* Corresponding author at: Department of Physics, Tsinghua University, Beijing 100084, China. Fax: +86 010 62772782.

0921-5093/$ – see front matter © 2012 Elsevier B.V. All rights reserved.
doi:10.1016/j.msea.2011.12.112

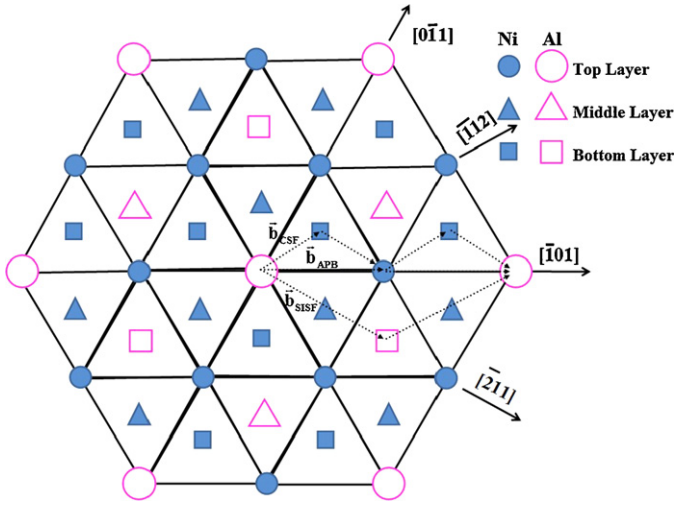

Fig. 1. Illustration of three successive (1 1 1) planes of Ni_3Al and the Burger's vectors of forming three kinds of planar faults. Filled blue figures stand for Ni atoms, open pink figures stand for Al atoms (For interpretation of the references to color in this figure legend, the reader is referred to the web version of the article).

the strength and ductility of Ni_3Al need to be evaluated, which is fundamental and essential for alloy design. In this paper, we perform first-principles calculations to explore the effects of Re, Ru, Ta, Ti and W on GSF energies, surface energies and Rice-criterion ductility in γ'-Ni_3Al. The results shed light on the strengthening mechanism of these alloying elements in Ni_3Al. We also explain the electronic mechanism underlying the effects via quantificational analyses of bonding strength between alloying elements and their neighbor atoms.

2. Computational method and models

Our DFT calculations were carried out with the plane-wave based Vienna ab initio simulation package (VASP) [25,26] using the projector augmented wave method [27,28] and the generalized gradient approximation in the parametrization by Perdew et al. [29]. Plane waves were included up to a cutoff energy of 350 eV, which yields convergent results. The convergence accuracy of the total energy was chosen as 10^{-5} eV in the relaxation of electronic degrees of freedom. The structures of the models were relaxed until the maximum force was less than 0.02 eV/Å. We used the Monkhorst–Pack scheme for k points sampling [30]. To calculate planar fault energies, we used supercells by introducing displacement on the (1 1 1). Ni_3Al is a close-packed structure with an arrangement of three successive planes along the <1 1 1> direction as shown in Fig. 1. An APB, CSF and SISF on the (1 1 1) plane were formed by shearing $a/2\langle\bar{1}\,0\,1\rangle(1\,1\,1)$, $a/6\langle\bar{1}\,\bar{1}\,2\rangle(1\,1\,1)$ and $a/3\langle\bar{2}\,1\,1\rangle(1\,1\,1)$ respectively. To eliminate the interactions of parallel faults, we introduced a vacuum region of 12 Å to separate the parallel faults. The supercells containing 12 layers along the <1 1 1> direction and 96 atoms in total, and the 16 atoms in the top and bottom layer are fixed during relaxation to avoid surface reconfiguration. An $8 \times 5 \times 1$ k-mesh was used for the k points sampling. Based on the hypothesis of dilute alloys, we set up a single-impurity model [7] to evaluate the effects of various alloying elements. In this model, one alloying element substitutes for an Al atom in the slip plane.

3. Results and discussion

Table 1 summarizes the unstable stacking fault energies in each slip system and alloying system. Fig. 2(a) shows the effects of alloying elements on GSF in the $\langle\bar{1}\,0\,1\rangle(1\,1\,1)$ slip system. From the

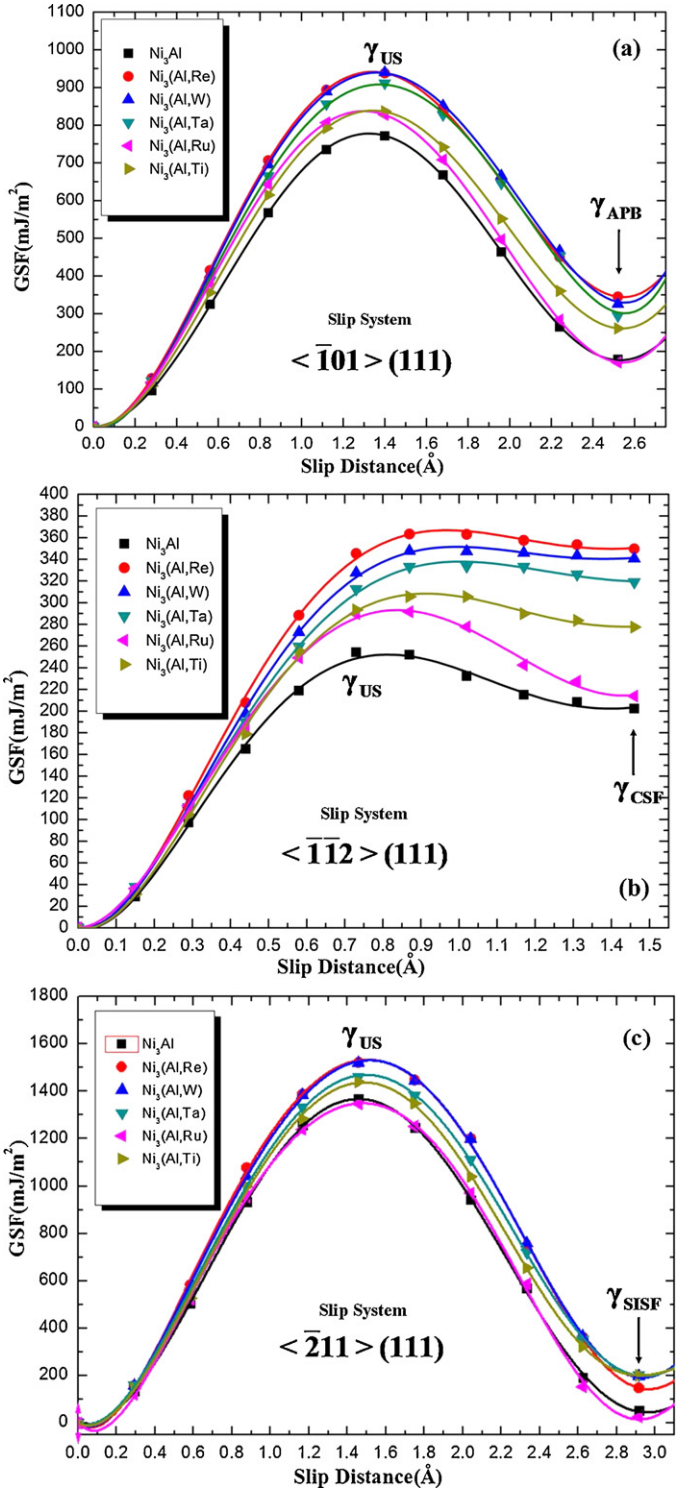

Fig. 2. The effects of alloying elements on the GSF energies in each slip system and alloying system.

results, we concluded that Re remarkably increases the unstable stacking fault energy in the $\langle\bar{1}\,0\,1\rangle(1\,1\,1)$ slip system of Ni_3Al. The abilities of other elements to raise the unstable stacking fault energies are in the order: W>Ta>Ti>Ru. The effects of alloying elements on GSF in the $\langle\bar{1}\,\bar{1}\,2\rangle(1\,1\,1)$ slip system in Fig. 2(b) are similar to those in the $\langle\bar{1}\,0\,1\rangle(1\,1\,1)$ system. Re promotes the unstable stacking fault energy most. Other alloying elements are also in the order: W > Ta > Ti > Ru. Fig. 2(c) presents the effects of alloying elements on GSF in the $\langle\bar{2}\,1\,1\rangle(1\,1\,1)$ slip system. The improvements of the unstable stacking fault energies caused by alloying elements are

Table 1
The effects of alloying elements on generalized stacking fault energies, surface energies and ductility parameters.

		Ni_3Al	$Ni_3(Al,Re)$	$Ni_3(Al,W)$	$Ni_3(Al,Ta)$	$Ni_3(Al,Ru)$	$Ni_3(Al,Ti)$
Surface energy	γ_s(mJ/m^2)	3705.10	4070.55	4124.42	4039.85	3798.86	3953.18
Slip system	γ_{us}(mJ/m^2)	777.75	941.30	939.45	907.87	837.20	838.61
$a/2\langle\bar{1}\,0\,1\rangle(1\,1\,1)$	$D=\gamma_s/\gamma_{us}$	4.76	4.32	4.39	4.45	4.54	4.71
Slip system	γ_{us} (mJ/m^2)	254.26	365.99	350.19	336.55	294.33	308.44
$a/6\langle\bar{1}\,\bar{1}\,2\rangle(1\,1\,1)$	$D=\gamma_s/\gamma_{us}$	14.57	11.12	11.78	12.00	12.91	12.82
Slip system	γ_{us} (mJ/m^2)	1367.90	1533.35	1531.30	1469.74	1349.66	1437.80
$a/3\langle\bar{2}\,1\,1\rangle(1\,1\,1)$	$D=\gamma_s/\gamma_{us}$	2.71	2.65	2.69	2.75	2.81	2.75

still in the order: Re > W > Ta > Ti. Ru decreases the unstable stacking fault energy. In conclusion, under the same concentrations, Re most effectively increases the unstable stacking fault energies in three slip systems of Ni_3Al. The unstable stacking fault energies represent the minimum energy barriers for partial dislocation nucleation. The higher the unstable stacking fault energy is, the more difficultly the dislocation emits and plastic deformation occurs. Thus, Re can improve the yield strength of Ni_3Al more than the other elements.

To examine how alloying alters the ductility of Ni_3Al we employ Rices analysis [15–18] of the competition between dislocation emission from a crack tip and crack cleavage. According to this model, we can conveniently define a dimensionless measure of ductility D to be the ratio of γ_s to γ_{us}, where γ_s is the energy needed to create two new (1 1 1) crack surfaces, γ_{us} is the unstable stacking fault energy in each slip system. The smaller the D is, the more likely the metal will tend to fail by cleavage fracture rather than shearing by dislocation mediated slip. The surface energies γ_s were obtained by first-principles calculations and the results of ductility D in various alloy and slip systems are listed in Table 1. From the results, the ductility parameters D of Ni_3Al(Re) are smallest in all three slip systems compared to other elements, which means Re induces more brittleness than the others besides improving the strength of Ni_3Al.

To gain a deeper insight into the origin of the strengthening effects of alloying elements, we quantifiably studied the interaction between atoms using a discrete variational method (DVM) [32,31]to calculate the static energy after the atomic configuration was relaxed by VASP. DVM is a numerical cluster method based on DFT. The molecular orbitals were expressed by a linear combination of atomic orbitals, and we used a single-site basis set with the frozen core mode in the atomic orbitals. We used the interatomic energy to describe the bonds between the atoms [33–35]. The interatomic energy between atom l and l' is derived:

$$E_{ll'} = \sum_n N_n \sum_{\alpha\alpha'} a^*_{n\alpha l} a_{n\alpha' l'} H_{\alpha' l'\alpha l}, \quad (1)$$

where N_n is the occupation number for molecular orbital Ψ_n, $H_{\alpha' l'\alpha l}$ is the Hamiltonian matrix element which connects the atomic orbital α' of atom l' to the atomic orbital α of atom l. The coefficient $a_{n\alpha l}$ is obtained from

$$a_{n\alpha l} = \langle \phi_{\alpha l} | \Psi_n(r) \rangle, \quad (2)$$

where $\phi_{\alpha l}$ is the wave function of the atomic orbital α of atom l. Since the $E_{ll'}$ is related to the Hamiltonian matrix element, it can reveal the interaction between adjacent atoms. A negative number with a large absolute value means a strong bond. The sum of interatomic energies between Al (or alloying element X) and its 12 first-nearest neighbor(FNN) atoms is

$$E_{\mathrm{FNN}} = \sum_{n=1}^{12} E_{ll'}[\mathrm{Al}(or\mathrm{X}) - \mathrm{Atom}_n^{\mathrm{FNN}}], \quad (3)$$

and the $E_{\mathrm{FNN}}^{\mathrm{Perfect}}$, $E_{\mathrm{FNN}}^{\mathrm{APB}}$, $E_{\mathrm{FNN}}^{\mathrm{CSF}}$ and $E_{\mathrm{FNN}}^{\mathrm{SISF}}$ were calculated in perfect Ni_3Al, APB region, CSF region and SISF region respectively and summarized in Table 2.

Because of the $L1_2$ structure, every Al site is surrounded by 12 FNN Ni atoms in perfect Ni_3Al, as shown in Fig. 3(a). $E_{\mathrm{FNN}}^{\mathrm{Perfect}}$ is the sum of interatomic energies between Al (or X) and its 12 FNN Ni atoms. The larger the absolute value of $E_{\mathrm{FNN}}^{\mathrm{Perfect}}$ is, the stronger the Al (or X)–Ni bonds are. Therefore, compared to Al in pure Ni_3Al all the alloying elements enhance the bonding with their FNN Ni atoms. The Re–Ni bonds are strongest because of the largest absolute value in all alloy systems. After forming the APB and CSF on the (1 1 1) plane, the FNN atoms of the Al site in the fault region become 11 Ni atoms and 1 Al atom, as shown in Fig. 3(b) and (c), respectively. The formation of an APB or CSF involves breaking an Al (or X) and Ni bond, and then producing an Al (or X) and Al bond. $E_{\mathrm{FNN}}^{\mathrm{APB}} - E_{\mathrm{FNN}}^{\mathrm{Perfect}}$ and $E_{\mathrm{FNN}}^{\mathrm{CSF}} - E_{\mathrm{FNN}}^{\mathrm{Perfect}}$ indicate the changes of interatomic energies induced by the deformations. The larger the values are, the more energies are needed to break Al (or X) and Ni bonds and form the fault regions; thus, the larger the GSF energies are. From the results, we see that the values of $E_{\mathrm{FNN}}^{\mathrm{APB}} - E_{\mathrm{FNN}}^{\mathrm{Perfect}}$ and $E_{\mathrm{FNN}}^{\mathrm{CSF}} - E_{\mathrm{FNN}}^{\mathrm{Perfect}}$ are largest in the Ni_3Al(Re) system, which means most of the energy is needed to break Re–Ni bonds and form the APB and CSF. Therefore, the largest unstable stacking faults energies are found in the Ni_3Al(Re) system.

In Fig. 3(d), after forming the SISF, the FNNs of Al remain 12 Ni atoms; however, the stacking fault is produced. $E_{\mathrm{FNN}}^{\mathrm{SISF}} - E_{\mathrm{FNN}}^{\mathrm{Perfect}}$ indicates the change of interatomic energies between Al (or X) and its 12 FNN Ni atoms before and after production of the SISF. The larger the value is, the higher the SISF energy is. The value of $E_{\mathrm{FNN}}^{\mathrm{SISF}} - E_{\mathrm{FNN}}^{\mathrm{Perfect}}$ in the Ni_3Al(Ta) system is largest and the value in the Ni_3Al(Ru) system is smallest. The results are in agreement with the highest SISF

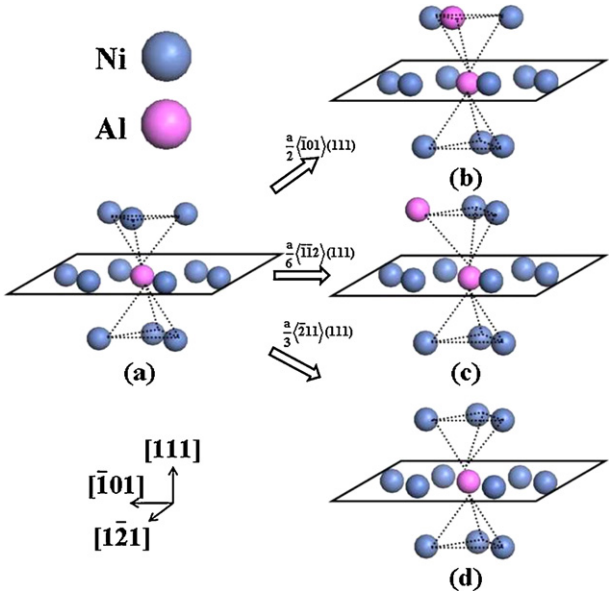

Fig. 3. The FNN atoms of Al site. (a) In perfect Ni_3Al. (b) In APB region. (c) In CSF region. (d) In SISF region. The blue balls stand for Ni atoms. The pink balls stand for Al atoms. (For interpretation of the references to color in this figure legend, the reader is referred to the web version of the article.)

Table 2
The effect of alloying elements on E_{FNN} in APB, CSF and SISF region.

Interatomic energy	Ni_3Al	$Ni_3(Al,Re)$	$Ni_3(Al,W)$	$Ni_3(Al,Ta)$	$Ni_3(Al,Ru)$	$Ni_3(Al,Ti)$
$E_{FNN}^{Perfect}$ (eV)	−7.66	−17.69	−14.53	−13.35	−8.75	−13.83
E_{FNN}^{APB} (eV)	−6.30	−16.09	−13.01	−11.84	−7.57	−12.4
E_{FNN}^{CSF} (eV)	−6.25	−14.74	−12.38	−11.31	−6.85	−11.92
E_{FNN}^{SISF} (eV)	−6.46	−16.28	−12.83	−11.62	−7.75	−12.12
$E_{FNN}^{APB} - E_{FNN}^{Perfect}$ (eV)	1.36	1.60	1.52	1.51	1.18	1.43
$E_{FNN}^{CSF} - E_{FNN}^{Perfect}$ (eV)	1.41	2.95	2.15	2.04	1.90	1.91
$E_{FNN}^{SISF} - E_{FNN}^{Perfect}$ (eV)	1.20	1.41	1.70	1.73	1.00	1.71

energy in the $Ni_3Al(Ta)$ system and the lowest SISF energy in the $Ni_3Al(Ru)$ system.

4. Summary

In summary, we used first-principles electronic structure calculations to study the influences of alloying elements on the GSF energies, strength and ductility of γ'-Ni_3Al. The abilities of the alloying elements to raise the GSF surface are in the order Re > W> Ta> Ti> Ru. Quantificational analyses of bonding strength show that the strong bonding of Re with its surrounding Ni atoms and weak bonding with its FNN Al atoms are the reason that Re increases the GSF more than other elements do. The unstable stacking fault energy represents the resistance to dislocation emitting. Hence, higher strengths can be obtained with higher unstable stacking fault energy, which reveals the mechanism by which alloying elements strengthen γ'-Ni_3Al. Meanwhile, Re increases brittleness of Ni_3Al most, which promotes the probability of cleavage fracture near crack tip.

Acknowledgment

Financial supports of the 973 Project (Ministry of Science and Technology of China, grant no. 2011CB606402) and the National Natural Science Foundation (Ministry of Science and Technology of China, grant no. 51071091) are gratefully acknowledged.

References

[1] R.C. Reed, The Superalloys Fundamentals and Applications, Cambridge University Press, 2006.
[2] E.A. Loria, Superalloy 718: Metallurgy and Applications, TMS, Warrendale, PA, 1989.
[3] T.M. Pollock, S. Tin, J. Propul. Power 22 (2006) 361.
[4] B.H. Kear, H.G.F. Wilsdorf, Trans. AIME 224 (1962) 382.
[5] V. Paidar, D.P. Pope, V. Vitek, Acta Metall. 32 (1984) 435.
[6] M.H. Yoo, Scripta metall. 20 (1986) 915.
[7] C.Y. Wang, S.Y. Liu, L.G. Han, Phys. Rev. B 41 (1990) 1359.
[8] D.J. Siegel, Appl. Phys. Lett. 87 (2005) 121901.
[9] G. Schoeck, S. Kohlhammer, M. Fahnle, Philos. Mag. Lett. 79 (1999) 849.
[10] G. Lu, N. Kioussis, V.V. Bulatov, E. Kaxiras, Phys. Rev. B 62 (2000) 3099.
[11] O.N. Mryasov, Y.N. Gornostyrev, M. van Schilfgaarde, A.J. Freeman, Acta Mater. 50 (2002) 4545.
[12] J.A. Yan, C.Y. Wang, S.Y. Wang, Phys. Rev. B 70 (2004) 174105.
[13] V. Vitek, Philos. Mag. A 18 (1968) 773.
[14] V. Vitek, Cryst. Lattice Defects 5 (1974) 1.
[15] J.R. Rice, J. Mech. Phys. Solids 40 (1992) 239.
[16] J.R. Rice, G.E. Beltz, J. Mech. Phys. Solids 42 (1994) 333.
[17] J.R. Rice, G.E. Beltz, Y.M. Sun, in: A.S. Argon (Ed.), Topics in Fracture and Fatigue, Springer, Berlin, 1992.
[18] Y.M. Sun, G.E. Beltz, J.R. Rice, Mater. Sci. Eng. A 67 (1993) 170.
[19] H. Van Swygenhoven, P.M. Derlet, A.G. Froseth, Nat. Mater. 3 (2004) 399.
[20] M. Muzyk, Z. Pakiela, K.J. Kurzydlowski, Scripta Mater. 64 (2011) 916.
[21] J. Han, X.M. Su, Z.H. Jin, Y.T. Zhu, Scripta Mater. 64 (2011) 693.
[22] R.C. Reed, A.C. Yeh, S. Tin, S.S. Babu, M.K. Miller, Scripta Mater. 51 (2004) 327.
[23] A. Mottura, N. Warnken, M.K. Miller, M.W. Finnis, R.C. Reed, Acta Mater. 58 (2010) 931.
[24] A. Volek, F. Pyczak, R.F. Singer, H. Mughrabi, Scripta Mater. 52 (2005) 141.
[25] G. Kresse, J. Hafner, Phys. Rev. B 47 (1993) 558.
[26] G. Kresse, J. Furthmuller, Phys. Rev. B 54 (1996) 11169.
[27] P.E. Blochl, Phys. Rev. B 50 (1994) 17953.
[28] G. Kresse, D. Joubert, Phys. Rev. B 59 (1999) 1758.
[29] J.P. Perdew, K. Burke, M. Ernzerhof, Phys. Rev. Lett. 77 (1996) 3865.
[30] H.J. Monkhorst, J.D. Pack, Phys. Rev. B 13 (1976) 5188.
[31] D.E. Ellis, G.A. Benesh, E. Byrom, Phys. Rev. B 16 (1977) 3308.
[32] B. Delley, D.E. Ellis, A.J. Freeman, E.J. Baerends, D. Post, Phys. Rev. B 27 (1983) 2132.
[33] C.Y. Wang, F. An, B.L. Gu, F.S. Liu, Y. Chen, Phys. Rev. B 38 (1988) 3905.
[34] F.H. Wang, C.Y. Wang, J.L. Yang, J. Phys.: Condens. Matter 8 (1996) 5527.
[35] F.H. Wang, C.Y. Wang, Phys. Rev. B 57 (1998) 289.